

# Proper Scaling of the Anomalous Hall Effect

Yuan Tian, Li Ye, and Xiaofeng Jin\*

*Surface Physics Laboratory and Physics Department, Fudan University, Shanghai 200433, China*

(Dated: November 9, 2018)

Working with epitaxial films of Fe, we succeeded in independent control of different scattering processes in the anomalous Hall effect. The result appropriately accounted for the role of phonons, thereby clearly exposing the fundamental flaws of the standard plot of the anomalous Hall resistivity versus longitudinal resistivity. A new scaling has been thus established that allows an unambiguous identification of the intrinsic Berry curvature mechanism as well as the extrinsic skew scattering and side-jump mechanisms of the anomalous Hall effect.

PACS numbers: 75.47.-m;75.47.Np;72.15.Eb;73.50.Jt

Shortly after the discovery of the Hall effect, in 1880 Edwin Hall further observed in ferromagnetic metals an additional large contribution besides the ordinary one, which is now called the anomalous Hall effect (AHE) - one of the most prominent phenomena existing in magnetic materials [1]. While the ordinary Hall effect has been well understood as a result of the Lorentz force deflecting the charge carriers, the mechanism of the AHE has remained controversial despite the long history of research, because its rich phenomenology defies the standard classification methodology, prompting conflicting reports claiming the dominance of various processes [2-12]. Recently it again attracts great attention because of its natural connection to the spin Hall effect and quantum spin Hall effect [13, 14].

In ferromagnets, the transverse resistivity has two contributions: one is ordinary and is proportional to the applied magnetic field; the other is anomalous and is normally proportional to the magnetization [8, 9]. It is often written as

$$\rho_{xy} = r_0 H + r_a M \equiv \rho_h + \rho_{ah} \quad (1)$$

where  $r_0$  and  $r_a$  are coefficients that characterize the strength of the ordinary and anomalous Hall resistivity  $\rho_h$  and  $\rho_{ah}$ , respectively. It has long been believed that  $\rho_{ah}$  should be a function of the longitudinal resistivity  $\rho_{xx}$  with well-defined material dependent parameters, i.e.,  $\rho_{ah} = f(\rho_{xx})$ .

However, despite the tremendous amount of experiments, a proper scaling between  $\rho_{ah}$  and  $\rho_{xx}$  has not yet been established. In general,  $\rho_{ah}$  could exhibit four types of behavior: (a)  $b\rho_{xx}^2$  (e.g. Fe) [15-18], (b)  $a\rho_{xx} + b\rho_{xx}^2$  (e.g. Co) [19, 20], (c)  $b\rho_{xx}^\alpha$  (e.g. Ni) with  $1 < \alpha < 2$  [21], and (d)  $a\rho_{xx}$  (e.g. ultra-pure Ni at low temperature) [22]. A unified picture that can explain all the diversifying experimental facts is currently absent.

Theoretically, Karplus and Luttinger first proposed that the spin-orbit interaction together with the interband mixing resulted in an intrinsic anomalous velocity in the direction transverse to the electric field [2], which gave  $\rho_{int} \propto \rho_{xx}^2$ . This intrinsic contribution to the AHE has been recently confirmed in the lan-

guage of Berry phase [10-12]. However, Smit suggested that the skew scattering at impurities was responsible for the AHE, which gave  $\rho_{sk} \propto \rho_{xx}$  [3]. Berger further proposed that another impurity-induced mechanism, the side-jump, could also give the  $\rho_{sj} \propto \rho_{xx}^2$  relation [5]. In contrast, recent first principles electronic band structure calculations based on the Berry phase interpretation suggested (although implicitly) that it is the Karplus-Luttinger intrinsic contribution rather than any impurity-induced extrinsic ones that plays the dominant role in the AHE [19, 23-25]. Apparently these predictions are contradictory to each other, while embarrassingly a direct experimental identification is still lacking. In a recent review by Sinitsyn [9], it is shown that the total anomalous Hall conductivity ( $\sigma_{ah}$ ) consists of five different microscopic contributions; they can be further divided into the above three categories in terms of the experimental identification by transport measurement, i.e.,  $\sigma_{ah} = \sigma_{int} + \sigma_{sk} + \sigma_{sj}$ , where  $\sigma_{int}$  is the intrinsic Karplus-Luttinger contribution and is irrelevant of any impurity,  $\sigma_{sk}$  is the extrinsic skew scattering that depends on the impurity density, and  $\sigma_{sj}$  the generalized extrinsic side-jump (including not only the conventional side-jump but also the contributions from intrinsic skew scattering and the anomalous distribution) that does not depend on the impurity density. It is a great challenge to separate the roles of intrinsic and extrinsic contributions in experiment.

Rising to these challenges we have developed a new experimental strategy that goes beyond the existing paradigms. Usually the longitudinal resistivity is taken as a quantity characteristic only of the material, so traditionally besides temperature,  $\rho_{xx}$  was varied only by changing the impurity concentration of the material. However, such an approach has the unavoidable defect that it would in fact modify not only the extrinsic but also the intrinsic contributions in the AHE, often complicating the interpretation of the experimental results. Instead, we are tuning the resistivity  $\rho_{xx}$  by varying the film thickness of ultrathin layer of Fe, an idea similar to the control of the coefficient of viscosity for a moving fluid in a thin tube by varying its diameter; the only

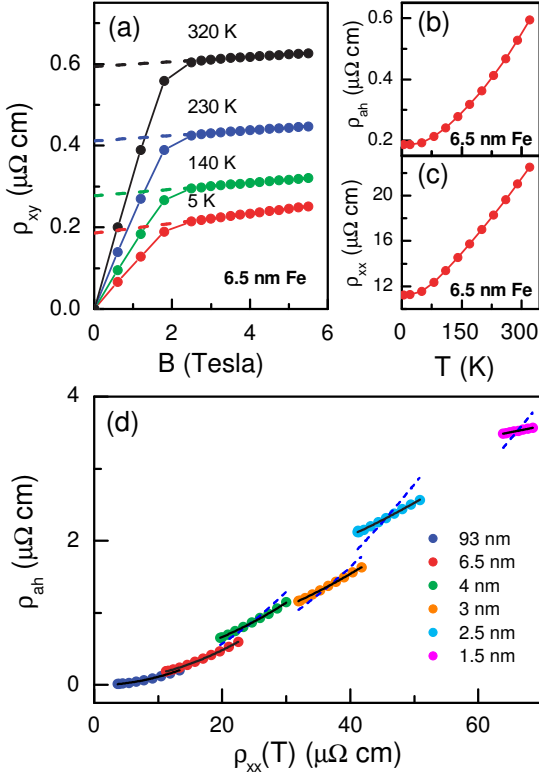


FIG. 1: (color online) (a) Experimentally measured representative  $\rho_{xy}$  vs  $H$  curves for 6.5 nm film, from which  $\rho_{ah}$  can be obtained. (b) and (c)  $\rho_{ah}$  and  $\rho_{xx}$  as functions of temperature for 6.5 nm film, respectively. (d)  $\rho_{ah}$  and  $\rho_{xx}$  for various film thicknesses. The dashed blue and solid black lines are fitting results with  $\rho_{ah} = b'\rho_{xx}^2$  and  $\rho_{ah} = a'\rho_{xx0} + a''\rho_{xx}T + b\rho_{xx}^2$ , respectively.

difference is that the former deals with electrons while the latter with molecules. It is this novel approach that helps appropriately account for the role of phonons in the impurity-originated scatterings, resulting in the proper scaling of the AHE:  $\sigma_{ah} = -(a_{sk}\sigma_{xx0}^{-1} + b_{sj}\sigma_{xx0}^{-2})\sigma_{xx}^2 + \sigma_{int}$  or  $\rho_{ah} = (a_{sk}\rho_{xx0} + b_{sj}\rho_{xx0}^2) - \sigma_{int}\rho_{xx}^2$ . Here  $\rho_{xx0}$  is the residual resistivity caused by defects in crystal,  $a_{sk}$  and  $b_{sj}$  are material dependent constants for the skew scattering and side-jump, respectively. This new scaling enables us to separate out the intrinsic Karplus-Luttinger contribution from the various impurity-originated extrinsic contributions, and further singles out its dominant role for the AHE as  $\sigma_{xx}^2 \rightarrow 0$ . We finally develop a unified physical picture that can explain all the previous experimental results.

Fe films were grown on undoped GaAs(001) at 300 K by molecular beam epitaxy (MBE), and were capped with 4 nm thick MgO to prevent oxidation in air. The detailed experimental setup was described elsewhere [26,

27]. The films were patterned into the form of a standard Hall bar along [110] with the magnetic field along [001]. The transport measurements were carried out in a physical property measurement system (Quantum Design PPMS-9T system). The magnetoresistance in Fe films at 5 Tesla is smaller than 0.5%, and the magnetization in Fe films thicker than 1 nm has its bulk value and changes little within the temperature range of 5 K-320 K.

The experimental relation between the anomalous Hall resistivity  $\rho_{ah}$  and the longitudinal resistivity  $\rho_{xx}$  is established through the following procedure. Fig. 1(a) shows several representative sets of  $\rho_{xy}$  vs  $H$  curves measured at different temperatures between 5 K and 320 K for a 6.5 nm thick Fe film.  $\rho_{ah}(T)$  is then obtained as the zero field extrapolation of the high field data as shown in the figure, and is displayed in Fig. 1(b).  $\rho_{xx}(T)$  was measured simultaneously and is shown in Fig. 1(c). From Fig. 1(b) and 1(c),  $\rho_{ah}$  versus  $\rho_{xx}$  curve for the 6.5 nm Fe film can be deduced and is displayed in Fig. 1(d), together with data for other thicknesses varying between 1.5 nm and 93 nm.

This experimentally established  $\rho_{ah} = f(\rho_{xx})$  at different film thicknesses provides an opportunity to unveil the phonon contribution to the AHE - a long-standing controversial issue [3, 6, 28]. Before going to the detailed data analysis, we recall first some very basics about the anomalous Hall effect. According to Ohm's law, there exists a general relation between the anomalous Hall resistivity and the anomalous Hall conductivity:  $\rho_{ah} = -\sigma_{ah}/(\sigma_{xx}^2 + \sigma_{ah}^2)$  or  $\sigma_{ah} = -\rho_{ah}/(\rho_{xx}^2 + \rho_{ah}^2)$ , which is material independent and is valid for each independent mechanism of the AHE. Since  $\sigma_{ah} \ll \sigma_{xx}$ ,  $\rho_{ah} \ll \rho_{xx}$ , and  $\sigma_{xx} = \rho_{xx}^{-1}$ , this can be further simplified to:  $\rho_{ah} = -\sigma_{ah}\rho_{xx}^2$  or  $\sigma_{ah} = -\rho_{ah}\sigma_{xx}^2$ . It immediately follows that different mechanisms are additive both in the anomalous Hall conductivity and resistivity, i.e.,  $\sigma_{ah} = \sum \sigma_j$  and  $\rho_{ah} = \sum \rho_j$  - an important fact that is quite often overlooked. Specifically, a constant  $\sigma_{int}$  therefore  $\rho_{int} = -\sigma_{int}\rho_{xx}^2$  is expected for any given material [2, 11, 12]; on the other hand, it was generally adopted without serious justification that the skew scattering and side-jump were expressed as  $\rho_{sk} = a_{sk}\rho_{xx}$  and  $\rho_{sj} = b_{sj}\rho_{xx}^2$  respectively. Following this line of reasoning, it seems quite natural why the formula  $\rho_{ah} = a_{sk}\rho_{xx} + b\rho_{xx}^2$  has been widely used to investigate the AHE and separate various contributions (e.g., [18, 19, 25]). But we are going to expose the fundamental flaws of this formula in the following, then establish a new scaling for the AHE.

Following the observation in bulk Fe reported in Ref. [15, 16], we used  $b'\rho_{xx}^2$  to fit the data in Fig. 1(d), but found the significant deviation when the Fe films were thinner than 6.5 nm, as clearly seen by the dashed lines in the figure. This means that the skew scattering must be considered in ultrathin Fe films although it is negligible in the bulk material. We therefore use the routinely accepted formula  $\rho_{ah} = a_{sk}\rho_{xx} + b\rho_{xx}^2$  to fit the data, but

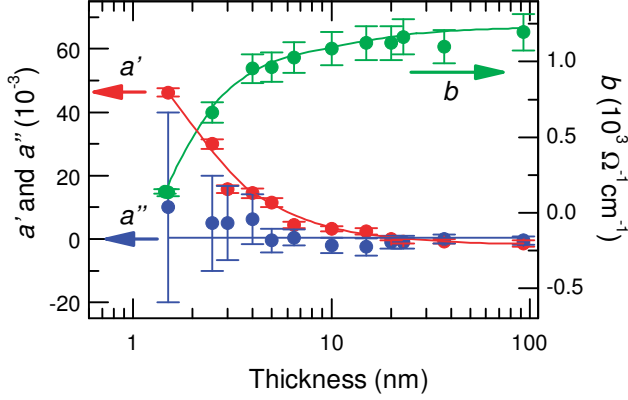


FIG. 2: (color online). Red, blue, and green dots represent respectively the parameters  $a'$ ,  $a''$  and  $b$ . Solid curves are guide to the eye.

found  $a_{sk}$  is not a constant, showing strong thickness dependence (not shown here). However since the impurity density concentration and the boundary condition remain the same for different film thickness, it is known that  $\rho_{xx}$  decreases as the film thickness increases, but it is puzzling why  $a_{sk}$  should be thickness dependent or  $\rho_{xx}$  dependent ( $a_{sk}(\rho_{xx})$ ). Unlike the experiments with variable impurity where  $a_{sk}(\rho_{xx})$  might happen, here in this new approach the fact that  $a_{sk}$  is not a constant strongly implies the improper scaling of the formula. We start to question why the skew scattering should be included as  $\rho_{sk} = a_{sk}\rho_{xx}$ . According to the Matthiessen's rule  $\rho_{xx} = \rho_{xx0} + \rho_{xxT}$  as seen in Fig. 1(c),  $\rho_{sk} = a_{sk}\rho_{xx}$  implies  $\rho_{sk} = a_{sk}\rho_{xx0} + a_{sk}\rho_{xxT}$ , i.e., the phonons would contribute (via  $\rho_{xxT}$ ) equally to the skew scattering just like the defects in crystal (via  $\rho_{xx0}$ ). This is certainly a very strong assumption and must be verified. In order to achieve this we first assume they contribute unequally to the skew scattering, i.e.,  $\rho_{sk} = a'\rho_{xx0} + a''\rho_{xxT}$ , then try to determine whether  $a'$  and  $a''$  are identical by fitting the data in Fig. 1(d) with  $\rho_{ah} = a'\rho_{xx0} + a''\rho_{xxT} + b\rho_{xx}^2$  using the experimentally measured  $\rho_{ah}$ ,  $\rho_{xx0}$ ,  $\rho_{xxT}$ , and  $\rho_{xx}$  for different film thicknesses, similar to those obtained for the 6.5 nm film in Fig. 1(b) and 1(c). The fits are shown by the solid lines in Fig. 1(d), and the fitting parameters of  $a'$ ,  $a''$  and  $b$  are presented in Fig. 2. It is evident from Fig. 2 that  $a'$  and  $a''$  are very different and actually  $a'' \approx 0$ . However, it seems that the same puzzle -  $a'$  is thickness dependent - still exists; it turns out that the two situations are fundamentally different, which becomes clear in the following.

Similarly, the same concern exists for the side-jump as well, i.e., why it should be included as  $\rho_{sj} = b_{sj}\rho_{xx}^2$  in the widely used formula, unlike in the intrinsic Karplus-Luttinger case where  $\sigma_{int}$  is a real constant so that  $\rho_{int} = -\sigma_{int}\rho_{xx}^2$  follows directly from the general rela-

tion between the anomalous Hall conductivity and resistivity. If the side-jump  $\rho_{sj} = b_{sj}\rho_{xx0}^2 + b_{sjT}\rho_{xxT}^2$  (it does not affect the following results even if there exists cross terms of  $\rho_{xx0}\rho_{xxT}$ ) is considered in parallel and together with the skew scattering  $\rho_{sk} = a_{sk}\rho_{xx0} + a_{skT}\rho_{xxT}$ , then without losing the generality what we should verify is  $\rho_{ah} = (a_{sk}\rho_{xx0} + a_{skT}\rho_{xxT}) + (b_{sj}\rho_{xx0}^2 + b_{sjT}\rho_{xxT}^2) - \sigma_{int}\rho_{xx}^2$ . It seems unreasonable from the first glance to work out so many parameters from Fig. 1(d) alone; however, the situation is dramatically changed when we regroup the formula in the form of  $\rho_{ah} = (a_{sk} + b_{sj}\rho_{xx0})\rho_{xx0} + (a_{skT} + b_{sjT}\rho_{xxT})\rho_{xxT} - \sigma_{int}\rho_{xx}^2$ , which has exactly one-to-one correspondence with the formula  $\rho_{ah} = a'\rho_{xx0} + a''\rho_{xxT} + b\rho_{xx}^2$  used to check the skew scattering above. Apparently we can reinterpret the same Fig. 2 as the following:  $a'' \approx 0$  is a direct experimental justification that phonons actually contribute little to the overall extrinsic AHE as compared to that of the defects in crystal, either the contributions from the skew scattering and side-jump cancels each other, or they are both negligible;  $b$  is nothing but the negative anomalous Hall conductivity  $b = -\sigma_{int}$ , which is fully developed and becomes almost saturated ( $b = -\sigma_{int} \approx 1.1 \times 10^3 \Omega^{-1} cm^{-1}$ ) as the film thickness reaches 4 nm and above; the thickness dependent  $a'$  in Fig. 2 simply indicates that the extrinsic AHE contains contributions not only from the skew scattering ( $a_{sk}\rho_{xx0}$ ) but also from the side-jump ( $b_{sj}\rho_{xx0}^2$ ) so that a thickness dependence  $a'$  should be expected as  $a' = (a_{sk} + b_{sj}\rho_{xx0})$ . Following this line of logic, a new scaling of  $\rho_{ah} = f(\rho_{xx}, \rho_{xx0})$  rather than the traditional  $\rho_{ah} = f(\rho_{xx})$  is proposed for the AHE:

$$\rho_{ah} = (a_{sk}\rho_{xx0} + b_{sj}\rho_{xx0}^2) - \sigma_{int}\rho_{xx}^2 \quad (2A)$$

$$\sigma_{ah} = -(a_{sk}\sigma_{xx0}^{-1} + b_{sj}\sigma_{xx0}^{-2})\sigma_{xx}^2 + \sigma_{int} \quad (2B)$$

Here,  $\sigma_{int}$ ,  $a_{sk}$  and  $b_{sj}$  are all material dependent constants.

To confirm indeed  $a' = (a_{sk} + b_{sj}\rho_{xx0})$ , i.e., the extrinsic anomalous Hall resistivity  $\rho_{ext} = a_{sk}\rho_{xx0} + b_{sj}\rho_{xx0}^2$  or anomalous Hall conductivity  $\sigma_{ext} = -(a_{sk}\sigma_{xx0}^{-1} + b_{sj}\sigma_{xx0}^{-2})\sigma_{xx}^2$  as in Eq. 2A and 2B, we plot in Fig. 3  $-\sigma_{ah0}$  vs  $\sigma_{xx0}$  as shown by the red dots, using the experimental raw data measured at 5 K for different film thicknesses. At this temperature, besides  $\rho_{xx0} = \sigma_{xx0}^{-1}$  we also have  $\sigma_{ah} \approx \sigma_{ah0}$  and  $\sigma_{xx} \approx \sigma_{xx0}$ , so that Eq. 2B becomes:  $-\sigma_{ah0} = a_{sk}\sigma_{xx0} + (b_{sj} - \sigma_{int})$ , by which the experimental data can be well fitted as seen from the black line in the figure, meanwhile the corresponding constants are extracted as:  $a_{sk} = -3.7 \times 10^{-3}$  and  $(b_{sj} - \sigma_{int}) = 1.8 \times 10^3 \Omega^{-1} cm^{-1}$ . Recalling the previous result  $-\sigma_{int} \approx 1.1 \times 10^3 \Omega^{-1} cm^{-1}$  from Fig. 2, we furthermore get the side-jump constant  $b_{sj} \approx 0.7 \times 10^3 \Omega^{-1} cm^{-1}$ . It is evident that at low temperatures the side-jump  $b_{sj}$  is not negligible comparing with the Karplus-Luttinger intrinsic term  $-\sigma_{int}$ ; on the other hand, the change of

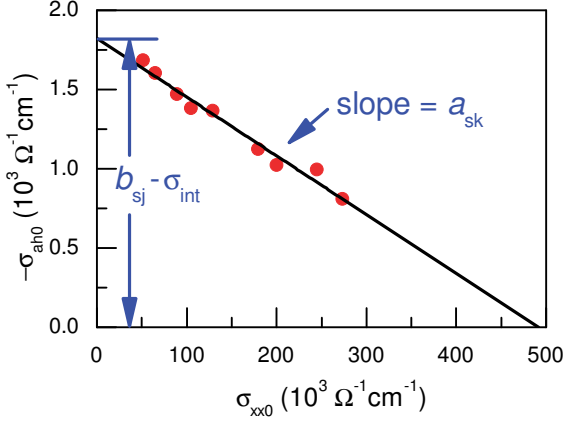


FIG. 3: (color online). The red dots represent the  $-\sigma_{ah0}$  vs  $\sigma_{xx0}$  relation using the experimentally measured raw data at 5 K for different film thicknesses. The black curve is the fitting by  $-\sigma_{ah0} = a_{sk}\sigma_{xx0} + (b_{sj} - \sigma_{int})$ .

$a_{sk}\sigma_{xx0}$  as a function of  $\sigma_{xx0}$  for the samples explored in this experiment as seen in Fig. 3 can be as large as  $1.0 \times 10^3 \Omega^{-1} cm^{-1}$ , almost the same magnitude of the  $-\sigma_{int}$  value, thus is also not small at all. In addition, the negative sign of  $a_{sk} = -3.7 \times 10^{-3}$  indicates that the skew scattering contributes to the AHE in Fe in the opposite direction as the side-jump and the Karplus-Luttinger terms do. Therefore in principle it could exceed them and becomes dominant at low temperature for samples with larger  $\sigma_{xx0}$ , explaining the striking and long puzzled phenomenon in which the anomalous Hall resistivity of Fe would change sign simply as the temperature is lowered as observed earlier [16], which was unable to understand with the simple  $\rho_{ah} = b'\rho_{xx}^2$  term.

Instead of the data fitting as done in Fig. 1(d) and Fig. 2, we are going to single out now the Karplus-Luttinger intrinsic contribution from the extrinsic contributions in a much more straightforward and transparent way. Fig. 4 shows the  $\sigma_{ah}$  versus  $\sigma_{xx}^2(T)$  plot using the experimental raw data, each curve corresponding to a specific film thickness with variable temperatures between 5 K and 290 K. This figure contains some important information about AHE, which has been hidden too long. First of all, the linear relationship between  $\sigma_{ah}$  and  $\sigma_{xx}^2$  confirms in an elegant way that phonons do contribute little to the skew scattering and side-jump in the AHE, as predicted by Eq. 2B, otherwise a linear relationship of  $\sigma_{ah}$  versus  $\sigma_{xx}$  would be expected from the widely used but flawed formula  $\rho_{ah} = a_{sk}\rho_{xx} + b\rho_{xx}^2$ . Then, as  $\sigma_{xx}^2$  goes to zero in the figure, the anomalous Hall conductivity  $\sigma_{ah}$  converges to essentially the same but nonzero value. This converged value is nothing but exactly the long searched Karplus-Luttinger intrinsic or the Berry curvature contribution, i.e.,  $\sigma_{ah} = (\sigma_{int} + \sigma_{sk} + \sigma_{sj}) \rightarrow \sigma_{int}$  when  $\sigma_{xx} \rightarrow 0$  according to Eq. 2B. To flesh out this criti-

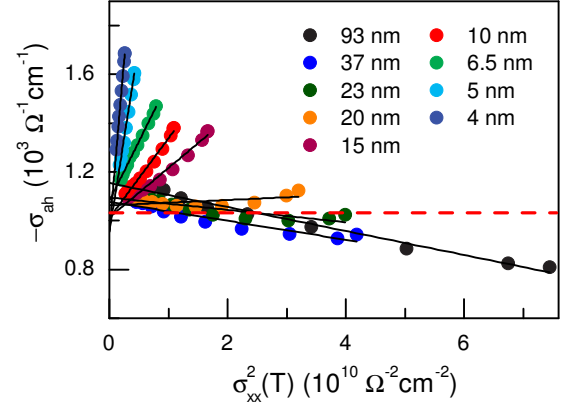


FIG. 4: (color online).  $-\sigma_{ah}$  vs  $\sigma_{xx}^2$  for Fe films with various thicknesses. The black lines are linear fitting of corresponding data. The red dashed line corresponds to the  $-\sigma_{ah}$  value obtained from iron whisker.

cal point, we believe that as  $\sigma_{xx}^2$  approaching zero (i.e. in the high temperature limit for metals), the extrinsic terms ( $\sigma_{sk} + \sigma_{sj}$ ) attributed to the impurity scattering ought to be washed out by the random and incoherent phonon scattering, therefore shrunk to zero as seen in Fig. 4; in the meantime, the intrinsic one of  $\sigma_{int}$  originated from the electronic structure of the material should be the only robust one that is usually less sensitive to temperature. In addition, this converged value of  $-\sigma_{int} \approx (1.1 \pm 0.1) \times 10^3 \Omega^{-1} cm^{-1}$  at  $\sigma_{xx}^2 = 0$  for films thicker than 4 nm not only agrees very well to the ( $b = -\sigma_{int}$ ) result of Fig. 2, but also to that from bulk Fe whisker measured at room temperature [16, 24] as marked by the red dashed line, which demonstrates unambiguously that it is the Karplus-Luttinger intrinsic rather than any extrinsic mechanisms that plays the dominant role for the AHE in bulk Fe at room temperature and higher. It should also be pointed out that for films thinner than 4 nm the  $-\sigma_{int}$  value decreases as seen in Fig. 2 (not shown in Fig. 4), presumably due to the finite-size or quantum-well modification (in ultrathin film of Fe) to the bulk electronic band structure.

With the new proper scaling of the anomalous Hall effect, Eq. 2A and 2B, we can now finally unify all the aforementioned diverse experimental results in literature. First, it is likely that type (a) as defined in the introduction corresponds to situations in which either the material dependent parameters  $a_{sk}$  and  $b_{sj}$  happen to be very small, or the measurements were carried out at temperatures where  $\rho_{xx0} \ll \rho_{xx}$ . Second, we have reanalyzed the data of type (b) using Eq. 2A, and found that the new scaling can indeed describe better those experimental results. Third, type (d) actually belongs to a special case of Eq. 2A where the temperature was fixed very low (so  $\rho_{xx} \approx \rho_{xx0}$ ) and the sample was ultra-pure (so

$\rho_{xx0}^2 \ll \rho_{xx0}$ ), thus the second and third terms in the equation are negligible compared to the first, leading to an equation of  $\rho_{ah} \approx a_{sk}\rho_{xx0}$ . Fourth, type (c) corresponds to a nontrivial case of Eq. 2A, where the intrinsic conductivity  $\sigma_{int}$  itself is sensitive to temperature in the range of interest [23, 24]. However, because of the absence of the Matthiessen's rule in semiconductors, it is not trivial whether the new scaling established here in Eq. 2 applies to the extrinsic AHE in magnetic semiconductors as well, although nothing is against it yet. Last but not least, if an experiment is carried out in a constant longitudinal current mode for an almost perfect ferromagnetic crystal at extremely low temperature, the anomalous Hall voltage is expected to be essentially zero according to Eq. 2A, but the anomalous Hall current is expected to be finite as seen from Eq. 2B.

We believe that the new result presented here opens wide possibilities to manipulate in a controlled way either intrinsic or extrinsic or both effects to meet certain application purposes in future spintronics devices.

This work was supported by MSTC (No. 2006CB921303 and No. 2009CB929203) and NSFC (No. 10834001).

---

\* Corresponding author, email: xfjin@fudan.edu.cn

- [1] E. H. Hall, Phil. Mag. 10, 301 (1880).
- [2] R. Karplus, J. M. Luttinger, Phys. Rev. 95, 1154 (1954).
- [3] J. Smit, Physica 24, 39 (1958).
- [4] J. M. Luttinger, Phys. Rev. 112, 739 (1958).

- [5] L. Berger, Phys. Rev. B 2, 4559 (1970).
- [6] The Hall Effect and Its Applications, edited by C. L. Chien and C. R. Westgate (Plenum, New York, 1980).
- [7] J. Sinova, T. Jungwirth, J. Cerner, Int. J. Mod. Phys. B 18, 1083 (2004).
- [8] N. Nagaosa, J. Phys. Soc. Jpn., 75, 042001, (2006).
- [9] N. A. Sinitsyn, J. Phys.: Cond. Matter, 20, 023201 (2008).
- [10] G. Sundaram and Q. Niu, Phys. Rev. B 59, 14915 (1999).
- [11] T. Jungwirth, Q. Niu, A. H. MacDonald, Phys. Rev. Lett. 88, 207208 (2002).
- [12] M. Onoda and N. Nagaosa, J. Phys. Soc. Jpn. 71, 19 (2002).
- [13] S. Murakami, N. Nagaosa, S.C. Zhang, Science 301, 1348 (2003).
- [14] B.A. Bernevig et al., Science 314, 1757 (2006).
- [15] W. Jellinghaus, M. P. DeAndres, Ann. Physik 7, 189 (1961).
- [16] P. N. Dheer, Phy. Rev. 156, 637 (1967).
- [17] W. L. Lee et al., Science 303, 1647 (2004).
- [18] Y. Pu et al., Phys. Rev. Lett. 101, 117208 (2008).
- [19] C. G. Zeng, Y. G. Yao, Q. Niu, H. H. Weitering, Phys. Rev. Lett. 96, 037204 (2006).
- [20] J. Kotzler, W. Gil, Phys. Rev. B 72, 060412(R) (2005).
- [21] J. Lavine, Phys. Rev. 123, 1273 (1961).
- [22] A. Fert, O. Jaoul, Phys. Rev. Lett. 28, 303 (1972).
- [23] Z. Fang et al., Science 302, 92 (2003).
- [24] Y. Yao, Q. Niu et al., Phys. Rev. Lett. 92 037204 (2004).
- [25] T. Miyasato et al, Phys. Rev. Lett. 99, 086602 (2007).
- [26] C. S. Tian, X.F. Jin et al., Phys. Rev. Lett. 94, 137210 (2005).
- [27] L. F. Yin, X.F. Jin et al., Phys. Rev. Lett. 97, 067203 (2006).
- [28] A. Crepieux and P. Bruno, Phys. Rev. B 64, 014416 (2001).